

A mouse model of the auditory nerve to study cochlear synaptopathy

Encina-Llamas, Gerard; Dau, Torsten; Harte, James Michael; Epp, Bastian

Publication date:
2018

Document Version
Publisher's PDF, also known as Version of record

[Link back to DTU Orbit](#)

Citation (APA):

Encina-Llamas, G., Dau, T., Harte, J. M., & Epp, B. (2018). A mouse model of the auditory nerve to study cochlear synaptopathy. Poster session presented at 41st MidWinter Meeting of the Association for Research in Otolaryngology, San Diego, United States.

DTU Library

Technical Information Center of Denmark

General rights

Copyright and moral rights for the publications made accessible in the public portal are retained by the authors and/or other copyright owners and it is a condition of accessing publications that users recognise and abide by the legal requirements associated with these rights.

- Users may download and print one copy of any publication from the public portal for the purpose of private study or research.
- You may not further distribute the material or use it for any profit-making activity or commercial gain
- You may freely distribute the URL identifying the publication in the public portal

If you believe that this document breaches copyright please contact us providing details, and we will remove access to the work immediately and investigate your claim.

Introduction

Several non-human animal studies have demonstrated a permanent loss of auditory nerve (AN) fiber synapses after noise over-exposure, termed cochlear synaptopathy, without causing hair cell loss nor altering normal auditory thresholds (e.g., Kujawa and Liberman, 2009). Studies in human listeners are generally inconclusive, mainly because assessing the status of the AN in humans represents a major challenge. In a previous study, we proposed the use of envelope following responses (EFR) as a tool to investigate synaptopathy both in mice and humans (Encina-Llamas *et al.*, under review; Parthasarathy *et al.*, 2017). Similar patterns in synaptopathic mice and humans were found. The use of a "humanized" version of the AN model by Zilany *et al.* (2009, 2014) could qualitatively account for the patterns obtained in the human listeners. Nevertheless, the use of the original animal version of the AN model (based on the cat) failed to simulate EFRs in mice. It was argued that a species-specific AN model could improve the non-human animal simulations. Given that the mouse is the most used and best characterized species in connection with cochlear synaptopathy, the present study proposes a modification of the original AN model by Zilany *et al.* (2009, 2014) based on cat data adapted to the mouse.

Aim of the project

- Modify the AN model by Zilany *et al.* (2009, 2014) based on the cat to adapt it to the mouse.
- Due to the complexity of the AN model, it was intentionally decided to modify as few parameters as possible.
- Three main blocks were modified: the middle-ear filter, the cochlear tuning ($Q_{10\text{ dB}}$ values), and the range of sensitive characteristic frequencies (CF).
- The ultimate goal was to use the model to simulate EFRs in non-synaptopathic and synaptopathic mice.

Methods

Model:

- "Mousified" version based on the AN model by Zilany *et al.* (2009, 2014).
- 200 characteristic frequencies (CF), ranging from 4.5 to 75 kHz.
- Synapses per IHC are simulated by several independent computations of each AN CF (30-60 fibers per CF with a total of 10000 fibers).
- Synaptopathy is simulated by computing a given CF less times..

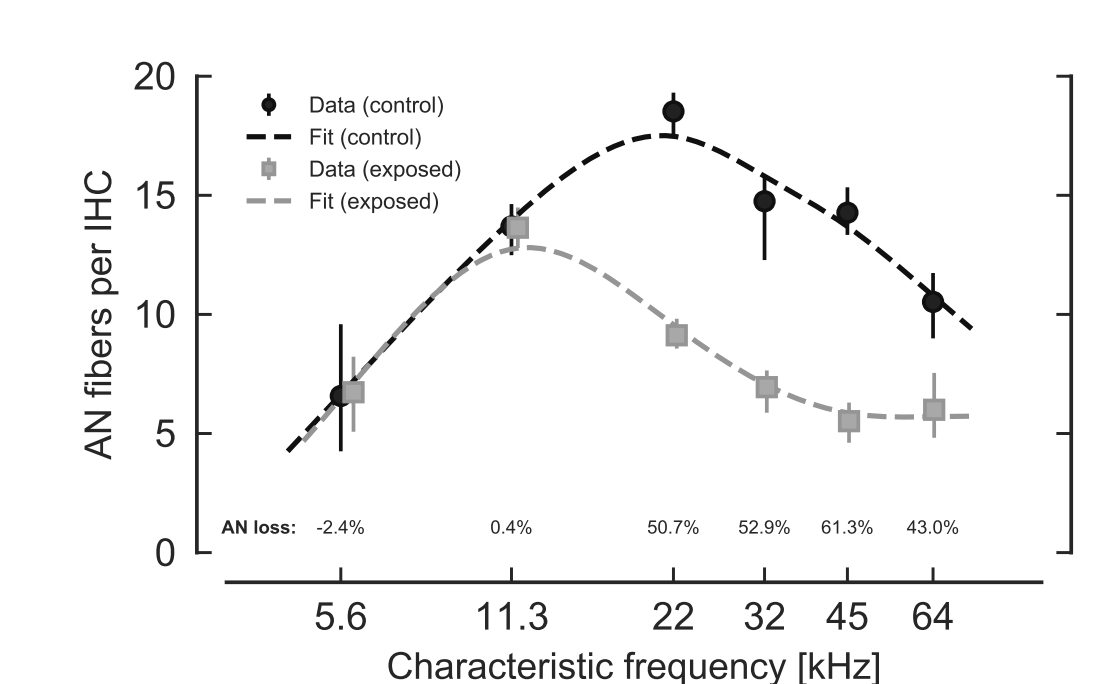


Fig. 1 Synaptic counts in the control (black) and exposed (gray) 32-week-old mice.

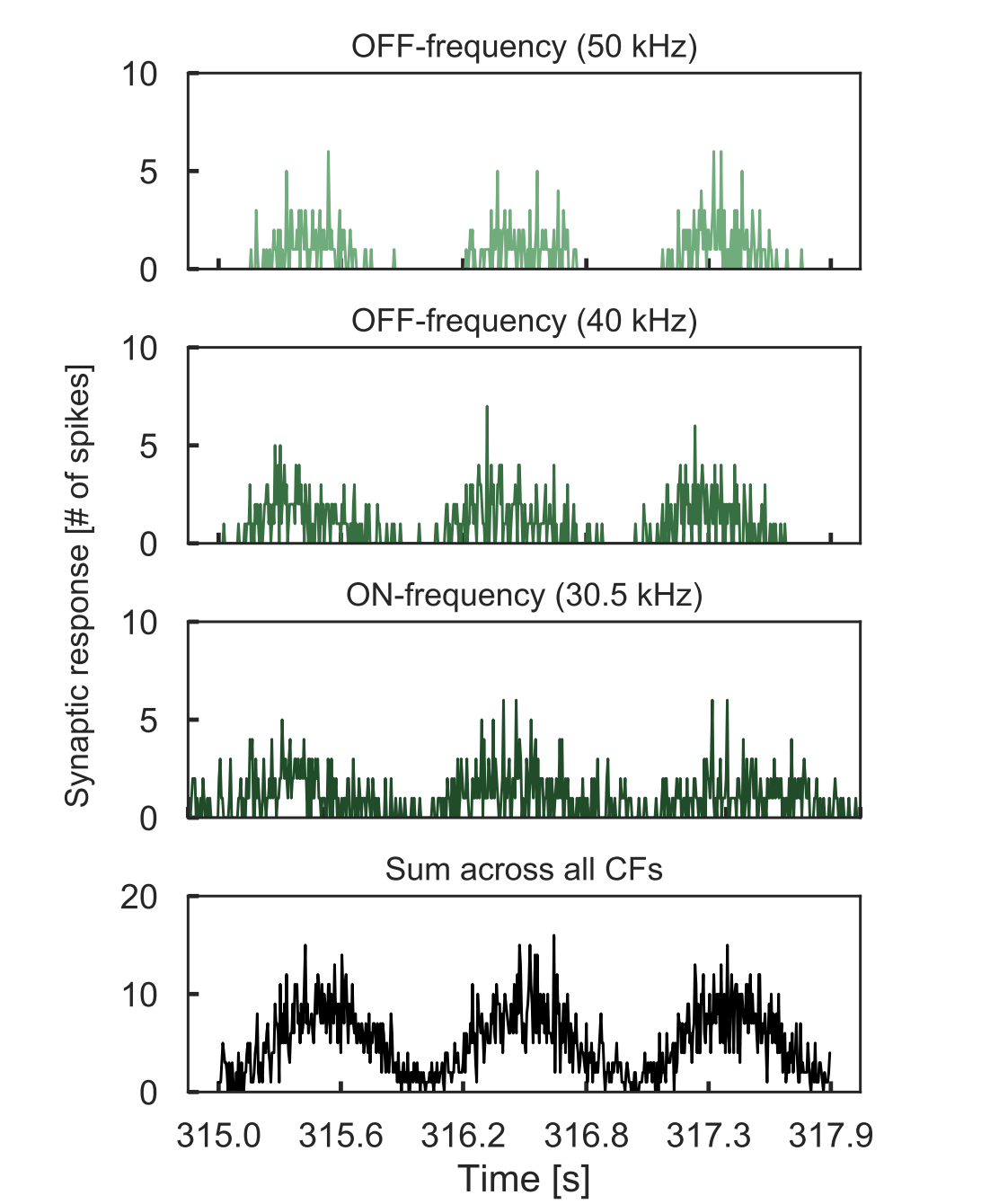


Fig. 2 Example of a simulated AN output at the synaptopathic frequency and level of 80 dB SPL.

Stimuli:

- Non-synaptopathic frequency: $f_c = 12.1$ kHz @ $f_m = 1024$ Hz
- Synaptopathic frequency: $f_c = 30.5$ kHz @ $f_m = 1024$ Hz

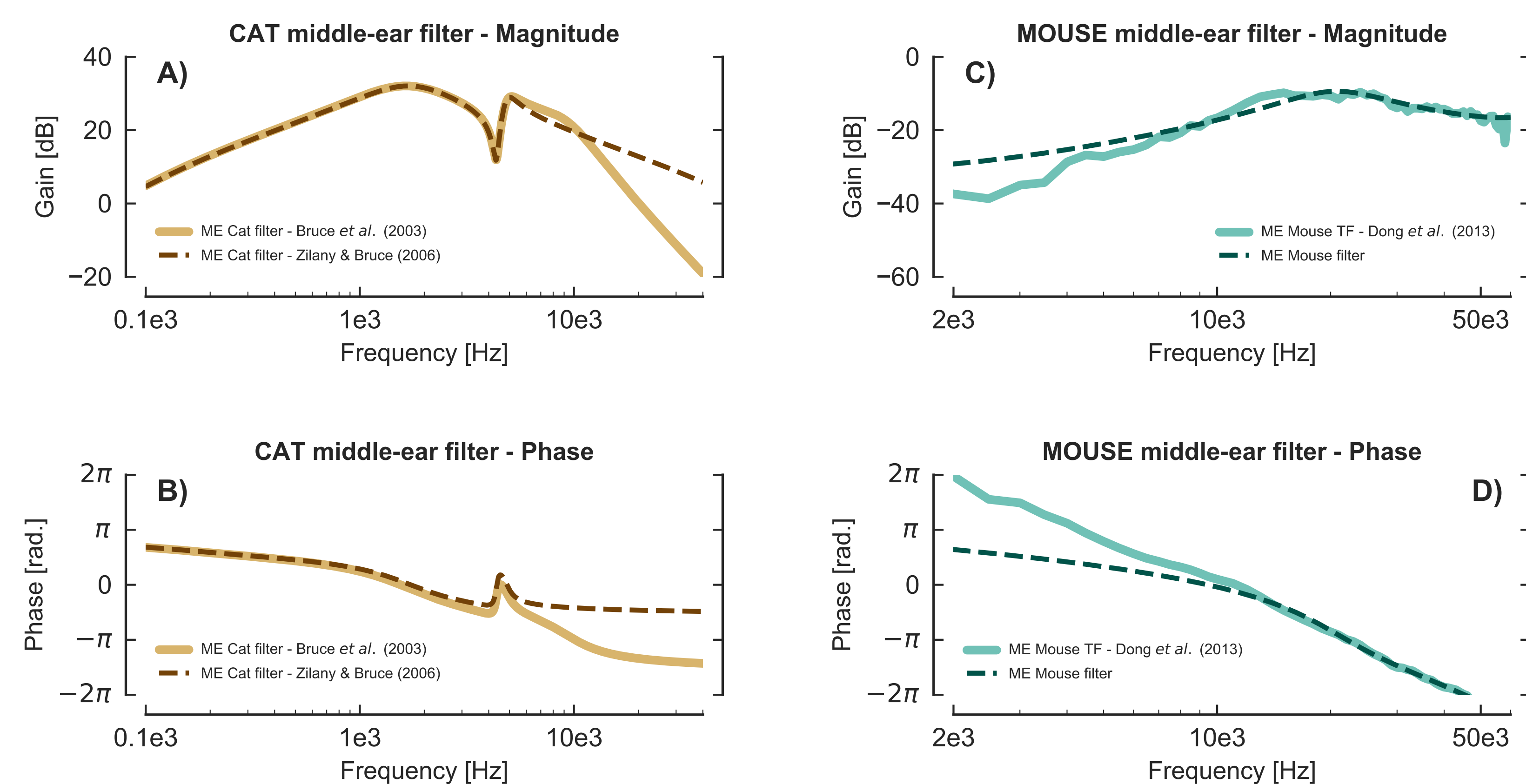
Levels:

- EFRs in mice: 20 to 80 dB SPL, 10 dB steps.
- Simulated EFRs: 10 to 100 dB SPL, 5 dB steps.

Modulations:

- Strong m = 85%; shallow m = 25%.

Middle-ear filter:



"Mousification" of the AN model

Fig. 3 Magnitude and phase responses of the middle-ear (ME) filters.

Panels A & B show the ME filters in the cat model. The solid lines correspond to the original 11th-order IIR filter in Bruce *et al.* (2003). The dashed lines correspond to the simplified 5th-order in a second-order section structure filter in Zilany & Bruce (2006). Panels C & D show the ME filter in the mouse model. The solid lines correspond to the measurement of the stapes velocity relative to the sound pressure at the eardrum of C57BL mice (Dong *et al.*, 2013). The dashed lines represent the ME filter designed based on the stapes measurement and adjusted to the 5th-order in a second-order section structure.

AN tuning:

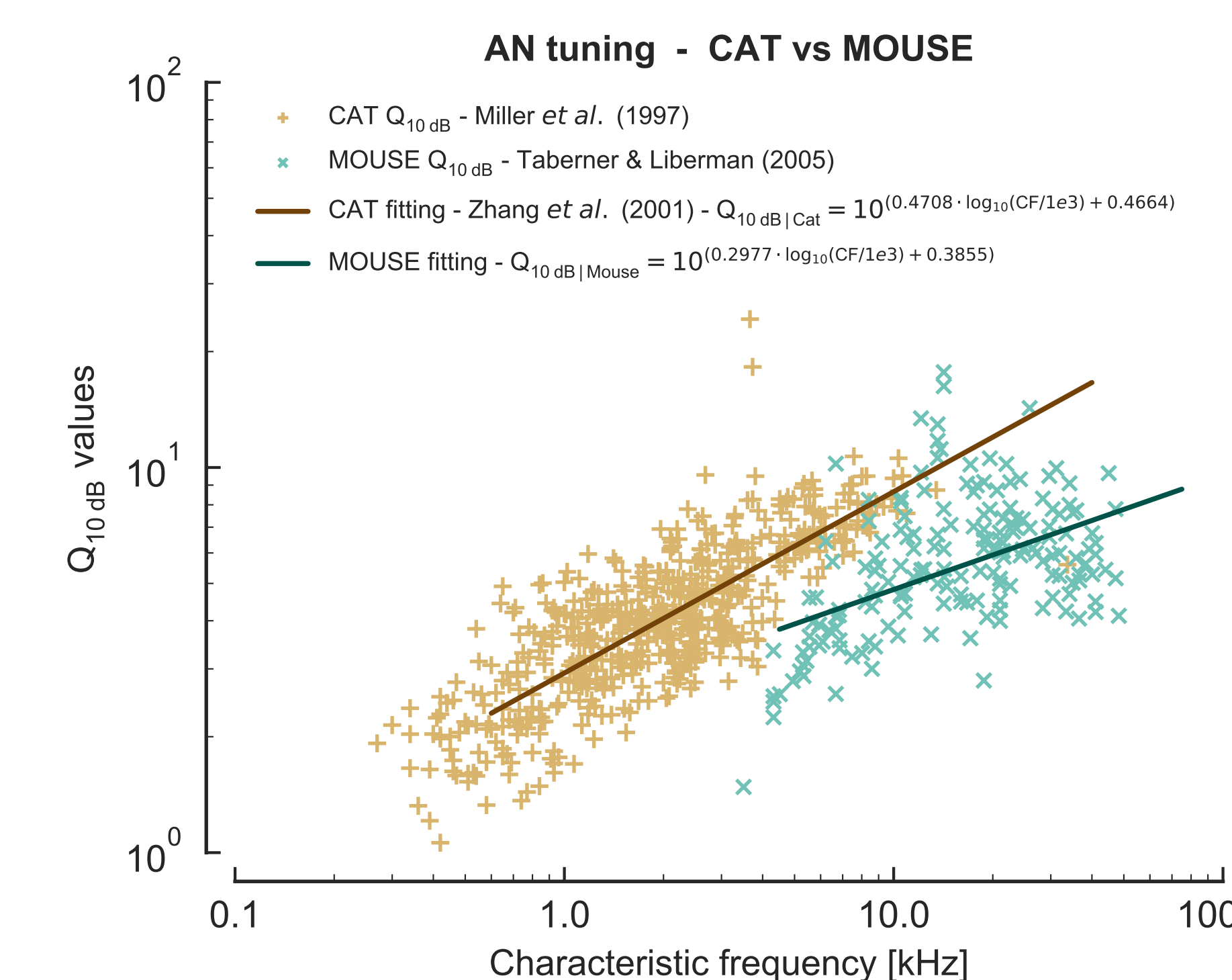


Fig. 4 AN tuning ($Q_{10\text{ dB}}$ values). Cat AN data (plus signs, Miller *et al.*, 1997) and fitted line (Zhang *et al.*, 2001) are represented in brown. Mouse (CBA/CaJ) AN data (crosses, Taberner & Liberman, 2005) and fitted line are represented in green.

AN threshold:

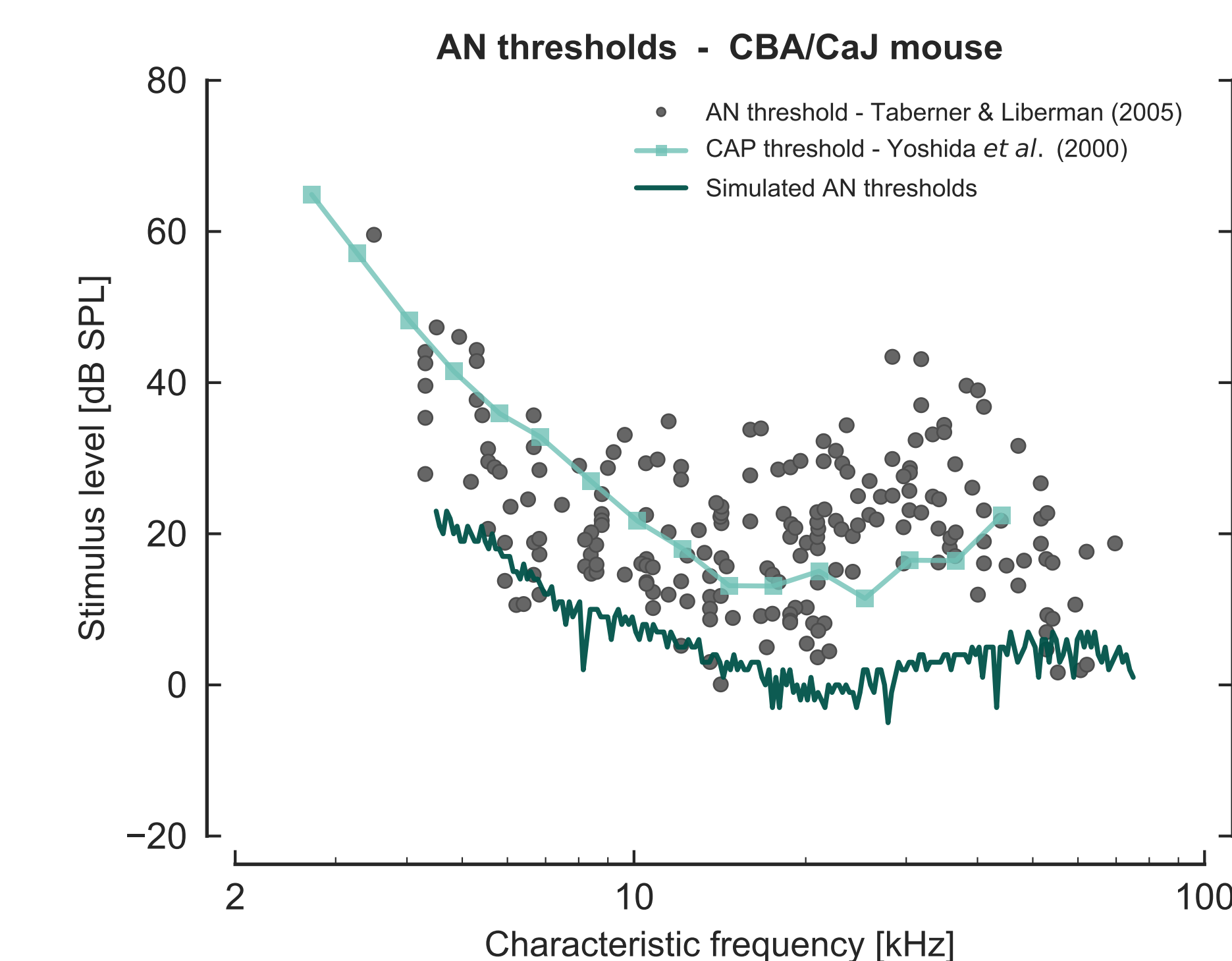


Fig. 5 Gray dots show AN threshold in CBA/CaJ mice (Taberner & Liberman, 2005). Light green squares compound action potential (CAP) thresholds in CBA/CaJ mice (Yoshida *et al.*, 2000). Dark green line shows simulated AN thresholds using the mouse model.

Results I

EFRs recorded in mice:

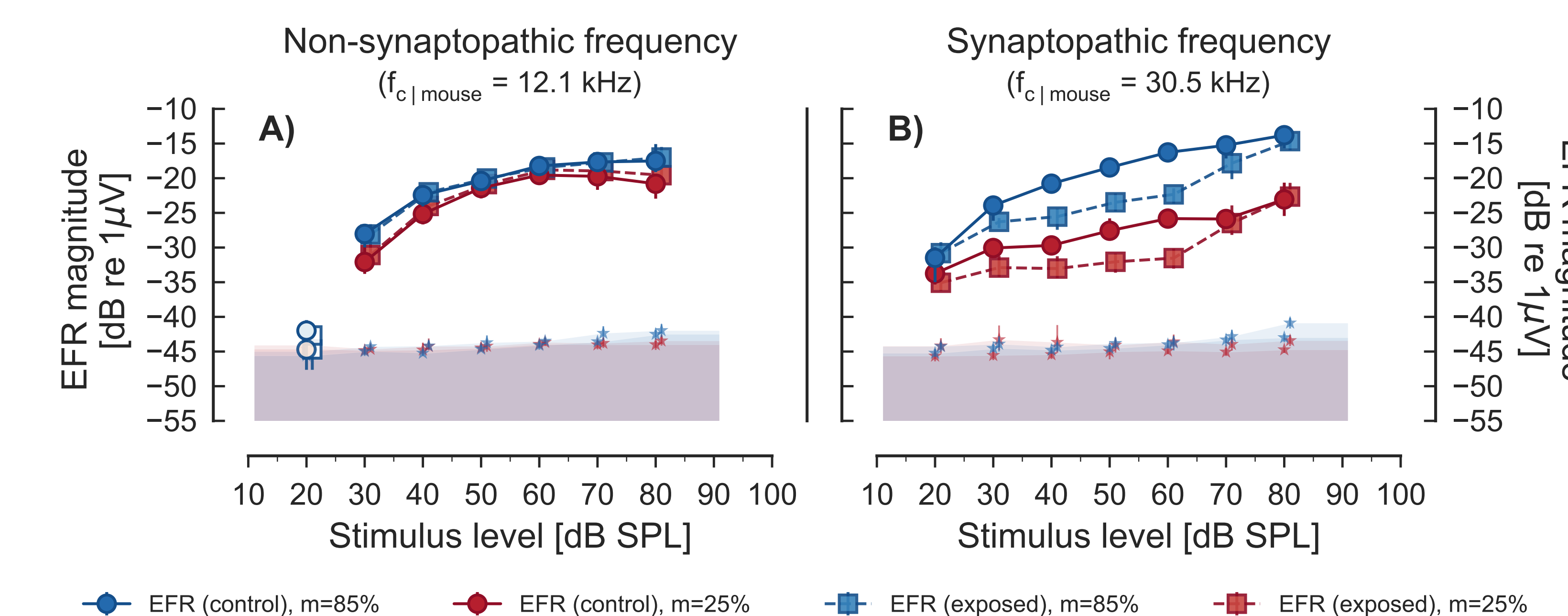


Fig. 6 EFR level-growth function recorded at the non-synaptopathic (Panel A, $f_c = 12.1$ kHz) and synaptopathic (Panel B, $f_c = 30.5$ kHz) frequencies for exposed (circles, solid lines) and non-exposed (squares, dashed lines) mice using strongly (blue) and shallowly (red) modulated tones. (For more information, attend to the podium PD 112 by Parthasarathy *et al.*, 2018).

Simulated EFRs using the CAT model:

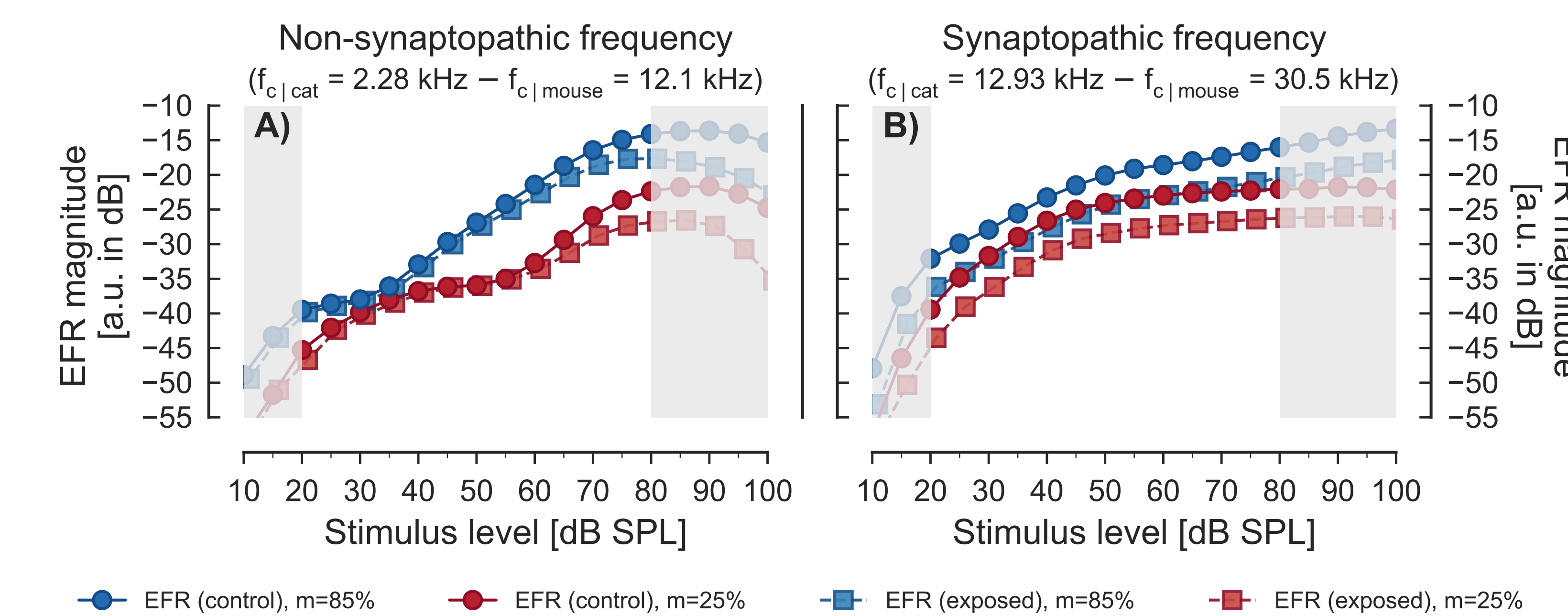


Fig. 7 Simulated AN EFR level-growth function using the CAT model at the non-synaptopathic (Panel A, $f_c = 2.28$ kHz) and synaptopathic (Panel B, $f_c = 12.93$ kHz) frequencies in the healthy (circles, solid lines) and the model with synaptic loss (squares, dashed lines) using strongly (blue) and shallowly (red) modulated tones.

Simulated EFRs using the MOUSE model:

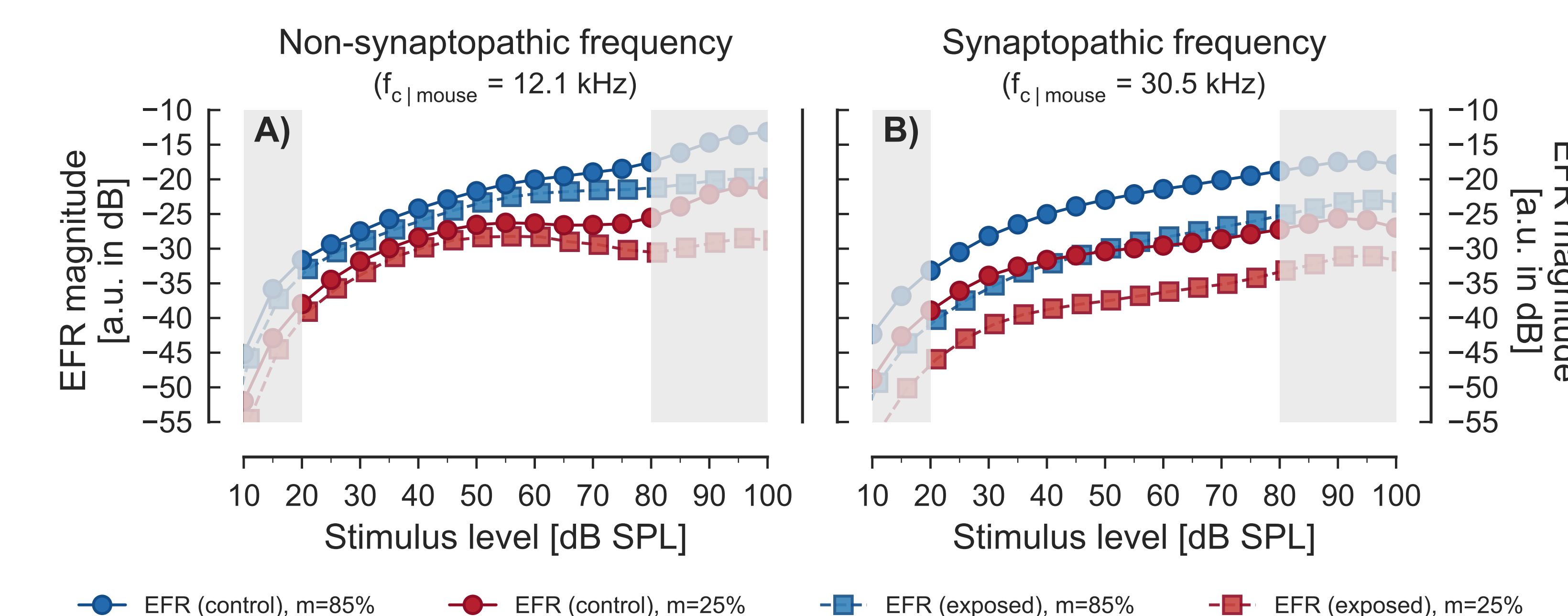


Fig. 8 Simulated AN EFR level-growth function using the MOUSE model at the non-synaptopathic (Panel A, $f_c = 12.1$ kHz) and synaptopathic (Panel B, $f_c = 30.5$ kHz) frequencies in the healthy (circles, solid lines) and the model with synaptic loss (squares, dashed lines) using strongly (blue) and shallowly (red) modulated tones.

Results II

Analysis at on- and off-frequencies and different fiber types:

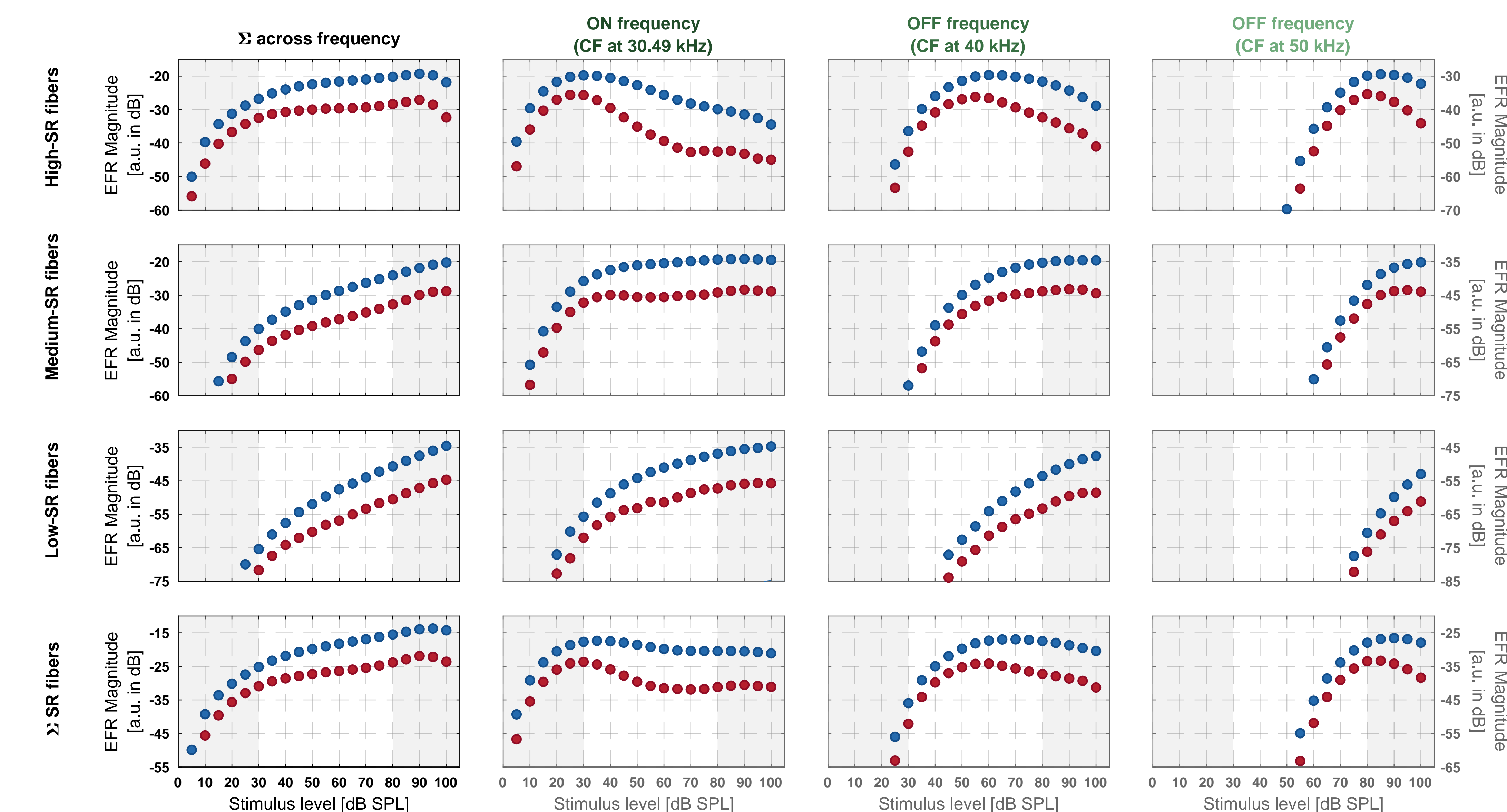


Fig. 9 Simulated EFR level-growth functions in the MOUSE model using strongly (blue) and shallowly (red) amplitude modulated tones. Rows show simulated EFRs for different types of AN fibers. Columns show simulated EFR level-growth functions at on- and off-frequencies.

Conclusion

- The modifications applied to "mousify" the AN model (ME filter, AN tuning and range of sensitive CFs) were sufficient to generally account for the mouse AN thresholds.
- The mouse model improved significantly the simulation of EFR level-growth functions in mice with respect to the use of the cat model.
- Although the model simulations capture the general trend of the EFR level-growth functions, there are still discrepancies in particular at the lower and higher stimulus levels at the synaptopathic frequency.
- Simulated EFRs using the mouse model at supra-threshold levels are dominated by the activity of high-SR fibers at off-frequency contributions, similarly to the humanized AN model (Encina-Llamas *et al.*, under review).

References

REFERENCES

- Bruce *et al.* (2003). *JASA*, 113(1), 369-388. DOI: 10.1121/1.1519544.
 Dong *et al.* (2013). *Hear Res*, 301:27-34. DOI: 10.1016/j.heares.2012.11.015.
 Encina-Llamas *et al.* (under review). *JARO*.
 Kujawa and Liberman (2009). *J. Neurosci.* 29(45), 14077-85. DOI: 10.1523/JNEUROSCI.2845-09.2009.
 Miller *et al.* (1997). *JASA*, 101(6), 3602-3616. DOI: 10.1121/1.418321
 Parthasarathy *et al.* (2017). *ARO MidWinter meeting*, 2017.
 Parthasarathy *et al.* (2018). *ARO MidWinter meeting*, 2018. PD 113.
 Taberner & Liberman (2005). *J. Neurophysiol.* 93(1), 557-69. DOI: 10.1152/jn.00574.2004.
 Yoshida *et al.* (2000). *Hearing Res.* 141(1-2), 97-106. DOI: 10.1016/S0378-5955(99)00210-5.
 Zhang *et al.* (2001). *JASA*, 109(2), 648-670. DOI: 10.1121/1.1336503.
 Zilany & Bruce (2006). *JASA*, 120(3), 1446-1466. DOI: 10.1121/1.2225512.
 Zilany *et al.* (2009, 2014). *JASA*, 126(5), 2390-412. DOI: 10.1121/1.3238250.

ACKNOWLEDGMENT

This research was supported by the Oticon Center of Excellence for Hearing and Speech Sciences (ChES5) at the Technical University of Denmark (DTU).